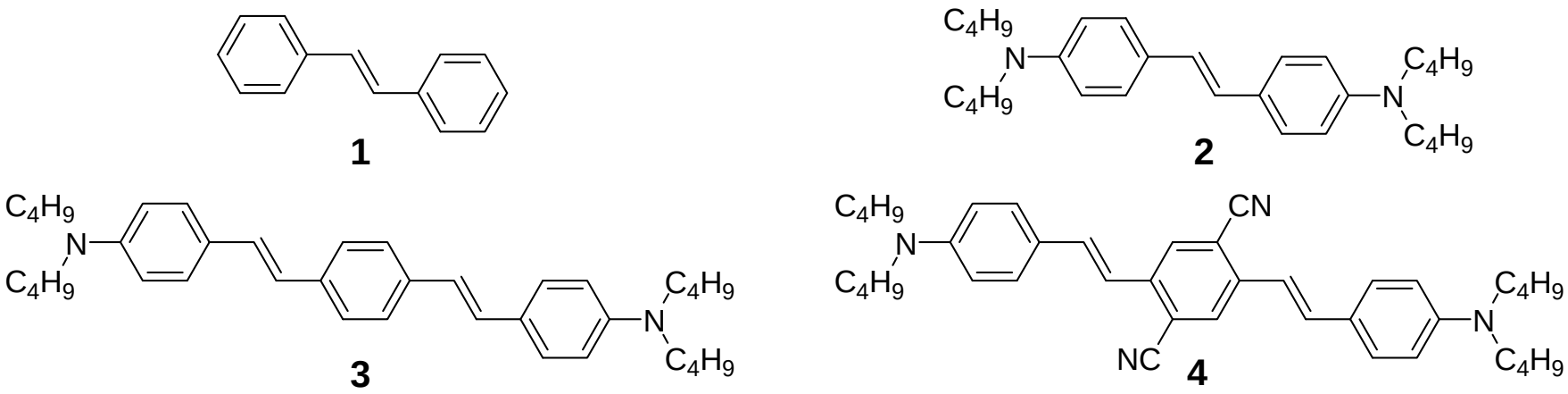

Figure 18.1 Structures of vinylene-phenylene type 2PA chromophores **1**-**4**.

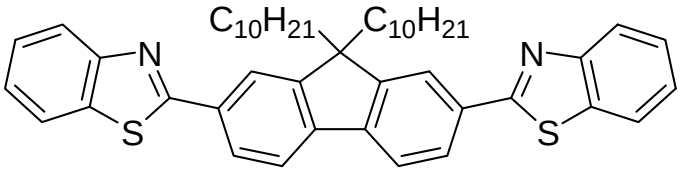

5

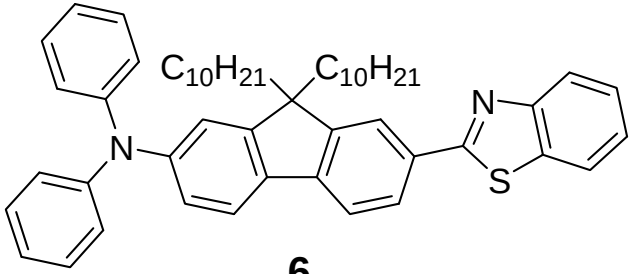

6

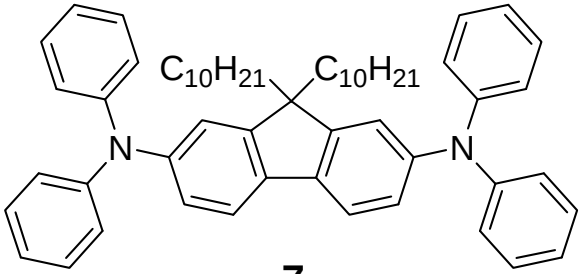

7

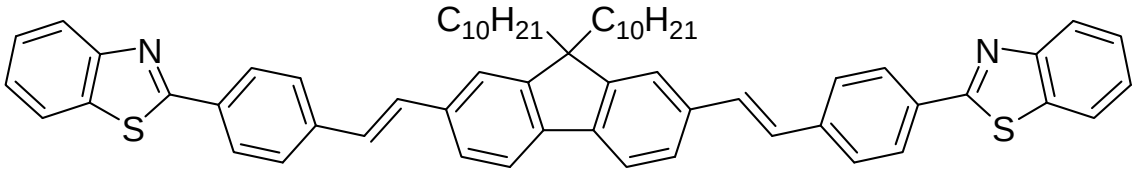

8

Figure 18.2 Structures of fluorene-based two-photon absorption (2PA) chromophores.

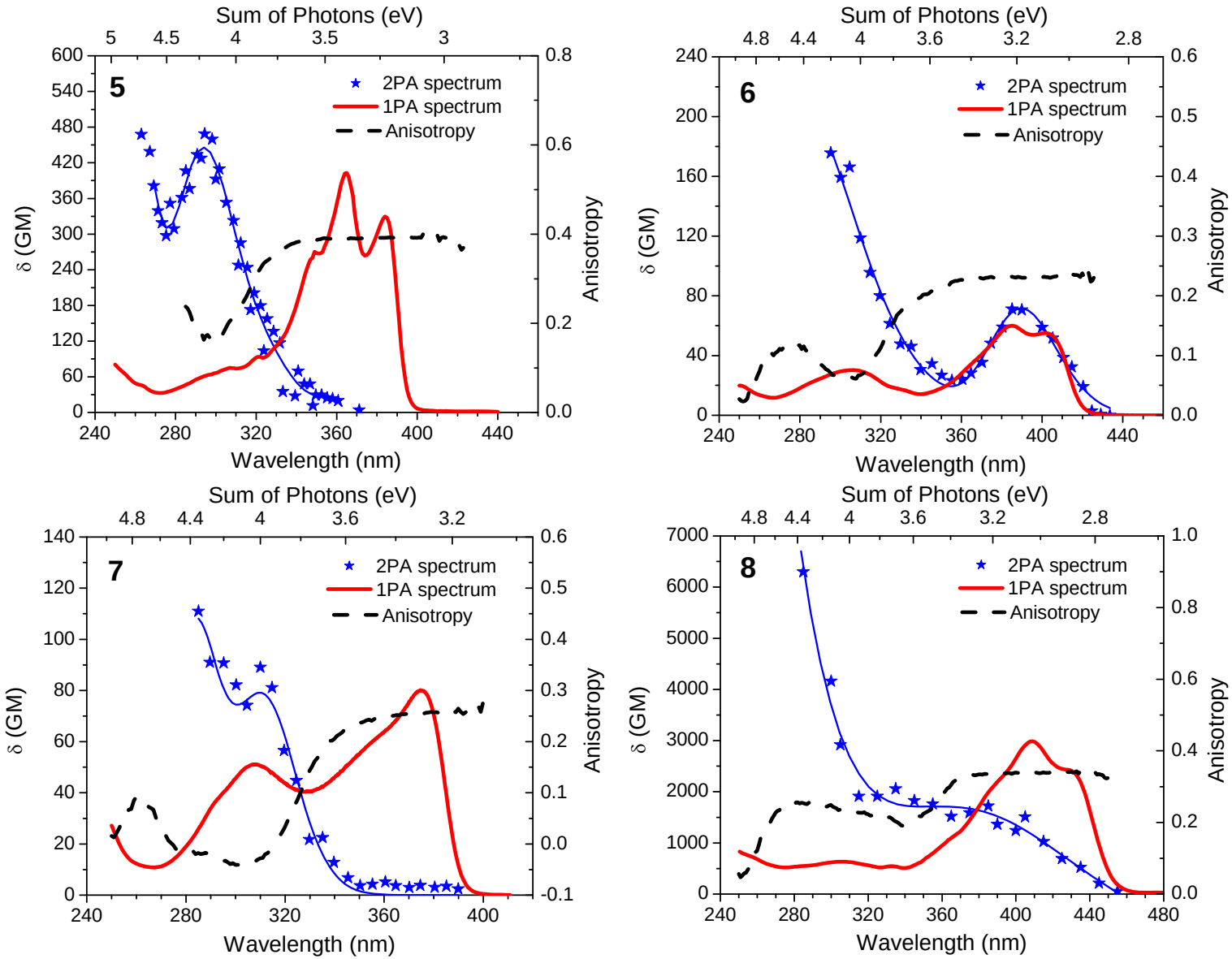

Figure 18.3 Linear absorption spectrum (red), steady-state excitation anisotropy, two-photon absorption of **5**-**8**.

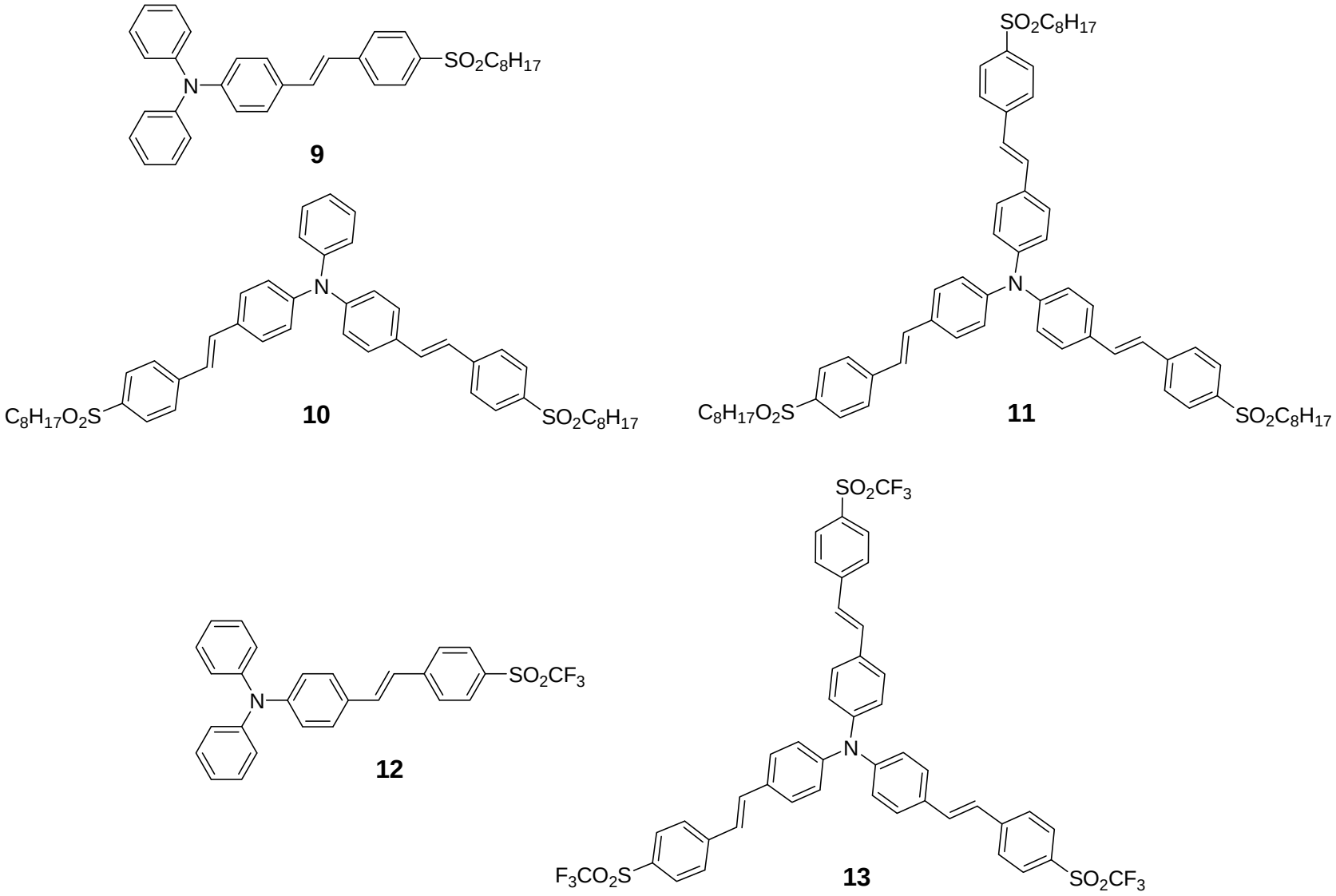

Figure 18.4 Structures of some branched molecules and their linear analogs.

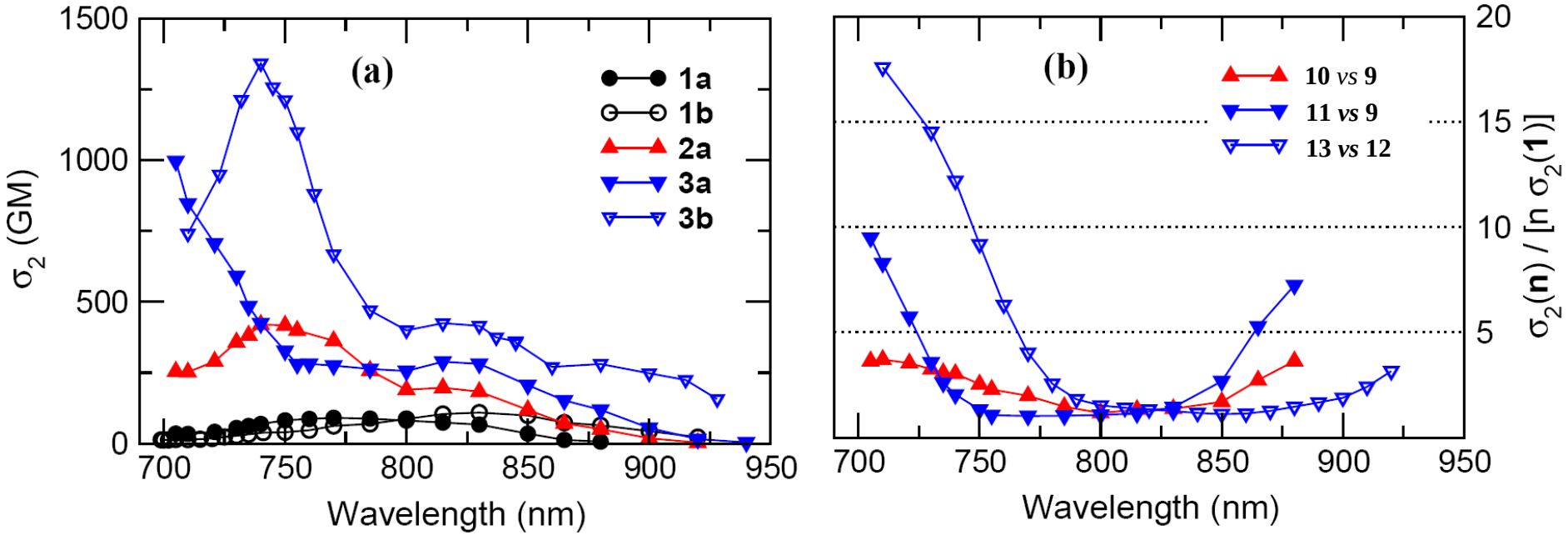

Figure 18.5 (a) Two-photon absorption (2PA) cross-sections of the investigated chromophores **9-13** in toluene. (b) wavelength dependence of the 2PA enhancement due to the branching effect.

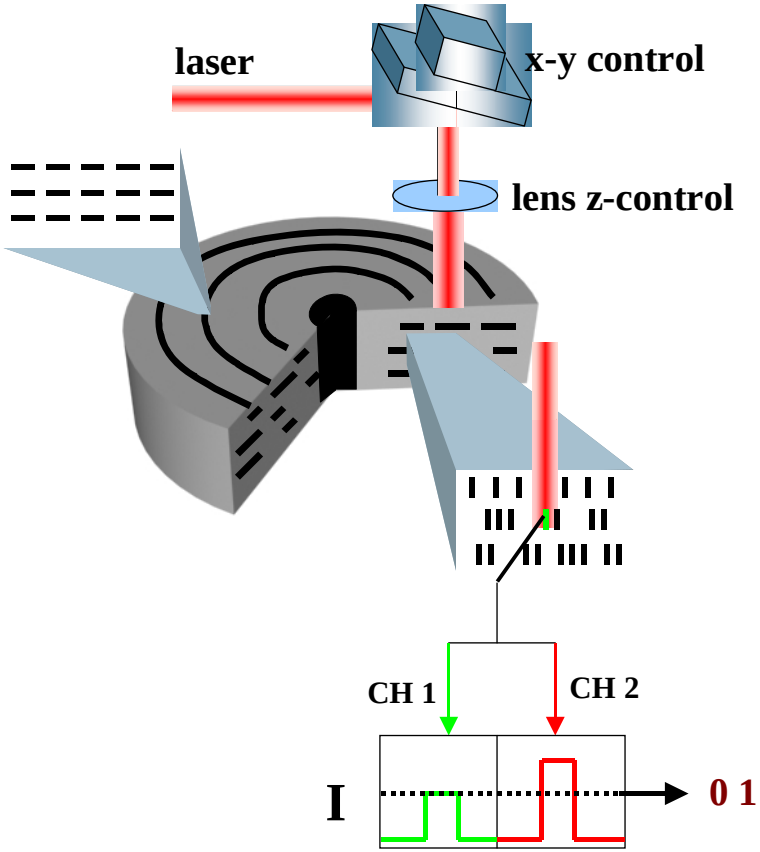

Figure 18.6 Multilayer two-photon three-dimensional (3D) optical data storage disk.

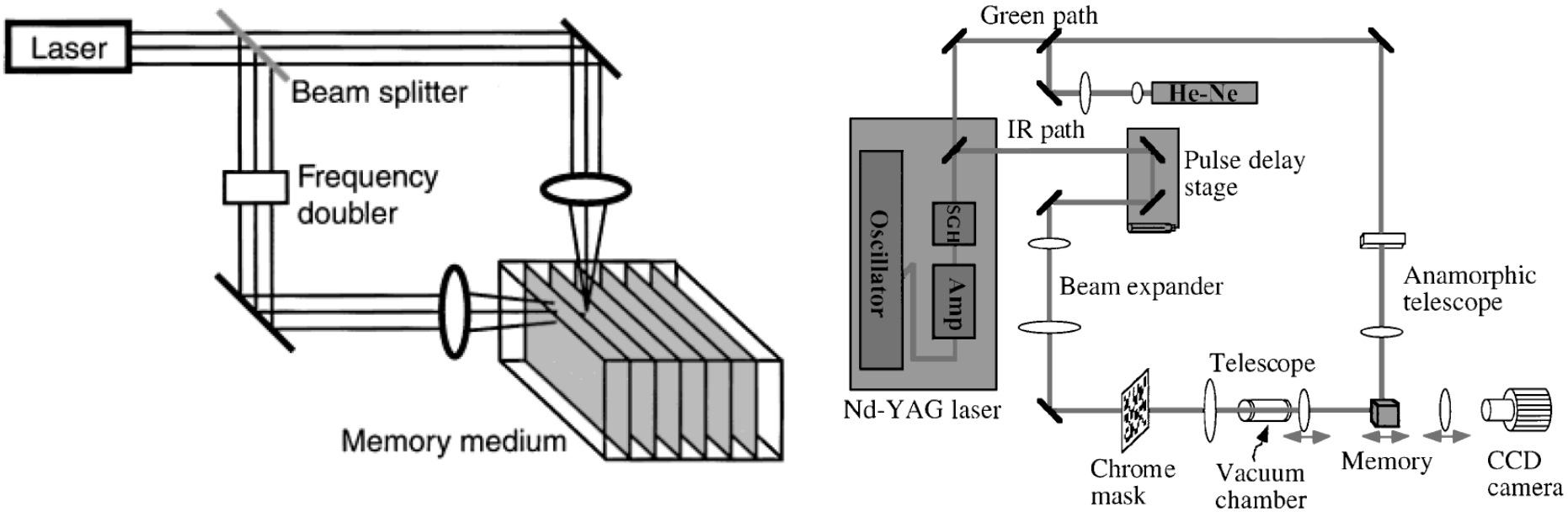

Figure 18.7 Principle of three-dimensional (3D) optical memories as proposed by Rentzepis *et al.*, and typical 3D data recording setup.

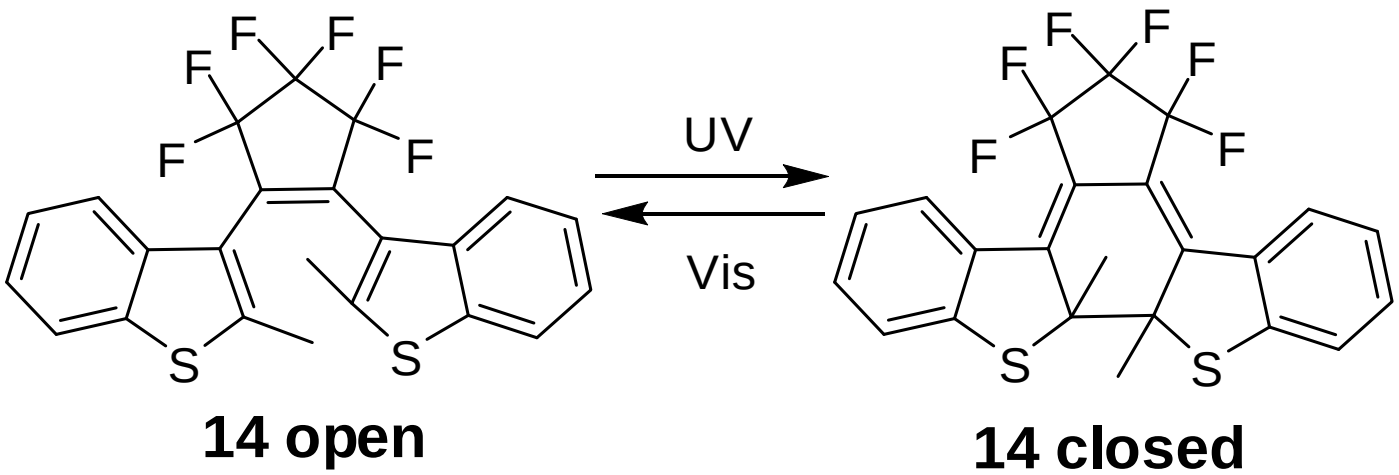

Figure 18.8 Molecular structures of the open and closed forms of the diarylethene **14.**

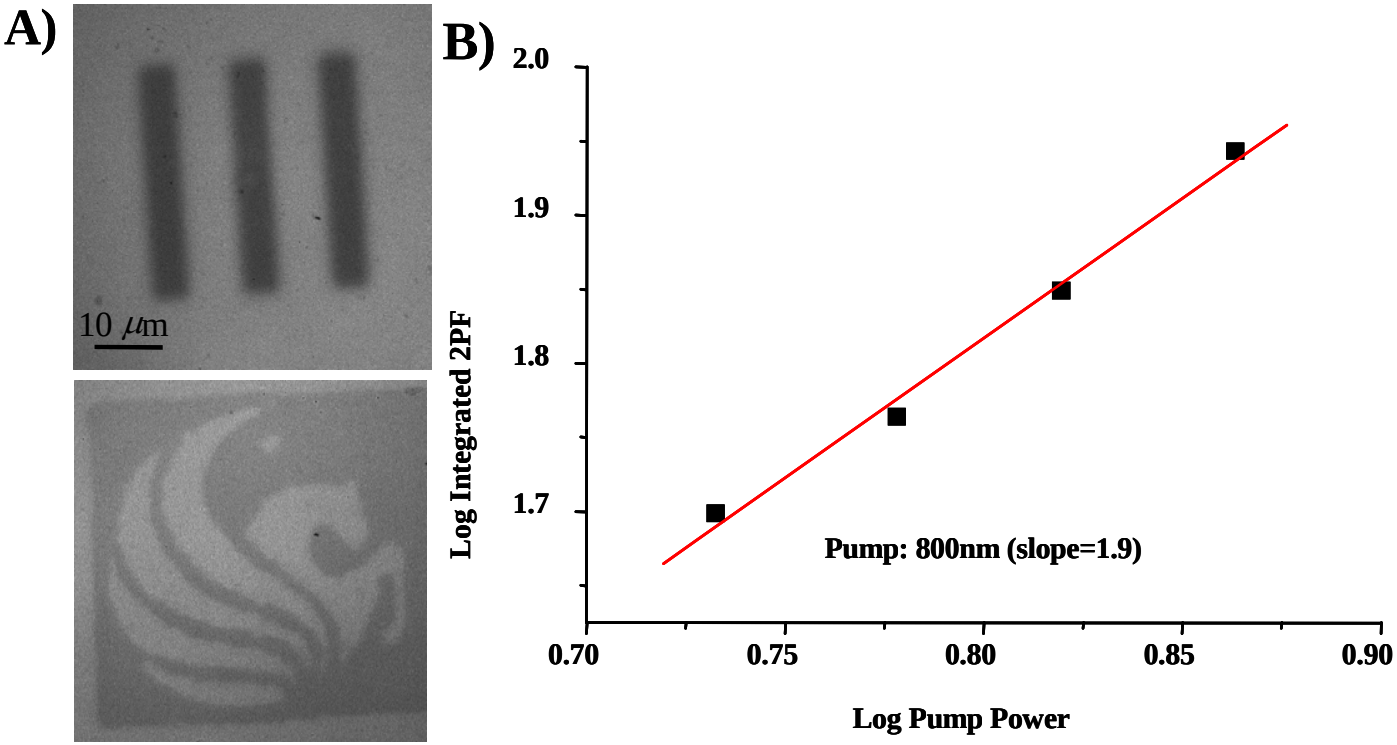

Figure 18.9 A) Two-photon fluorescence (2PF) readout patterns. The readout wavelength λ_{exc} is 800 nm (corresponding to 400 nm of single-photon excitation [1PE]). Upconverted fluorescence emission of fluorene **8** was collected between 510 and 550 nm and b) The plot shows quadratic dependence of integrated fluorescence emission intensity on several pump powers, which confirms the readout signal is due to the 2PF.

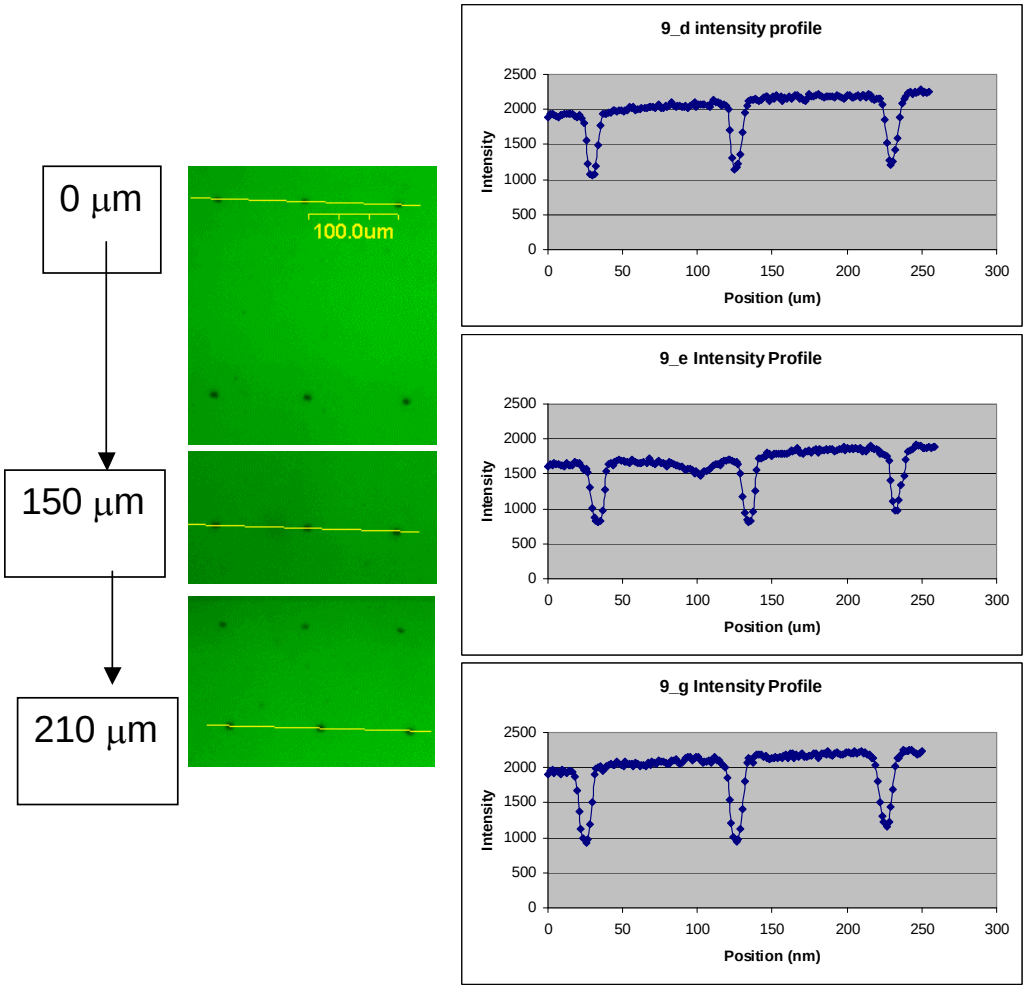

Figure 18.10 Multilayer, two-photon three-dimensional (3D) data recording and readout in a photosensitive polymer film containing a sulfonium salt and dye **6**. Recording (540 nm) and readout (800 nm) were conducted using femtosecond irradiation. The numbers on the left indicate the relative position in the z direction (depth) of the three layers. Data tracks are in the center with the line in yellow indicating the data that was readout in the fluorescence intensity plots on the right.

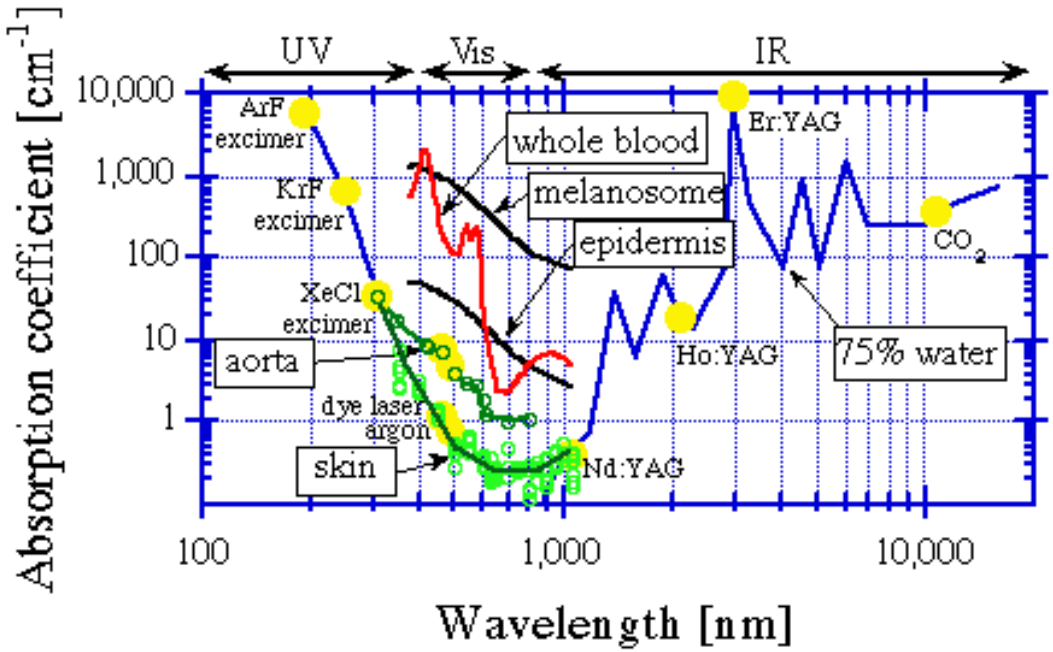

Figure 18.11 Primary absorption spectra of biological tissues along with their absorption coefficients at some common laser wavelengths.

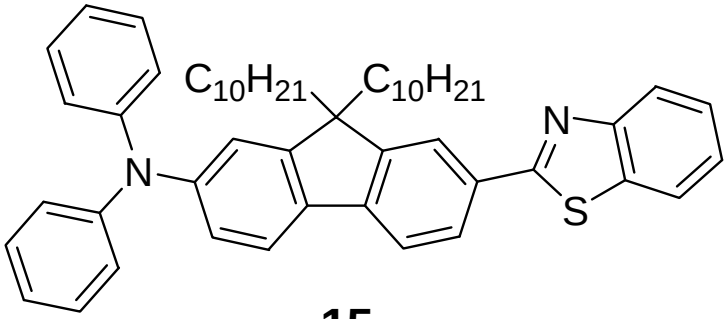

15

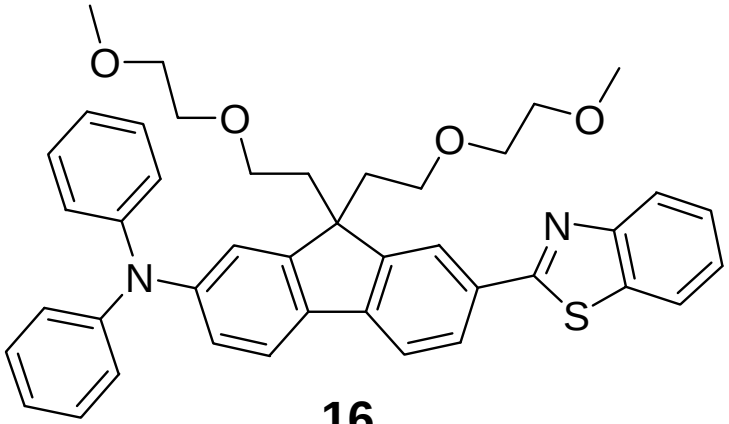

16

Figure 18.12 Structures of two-photon absorption (2PA) fluorescent probe with different hydrophilicities **15** and **16**.

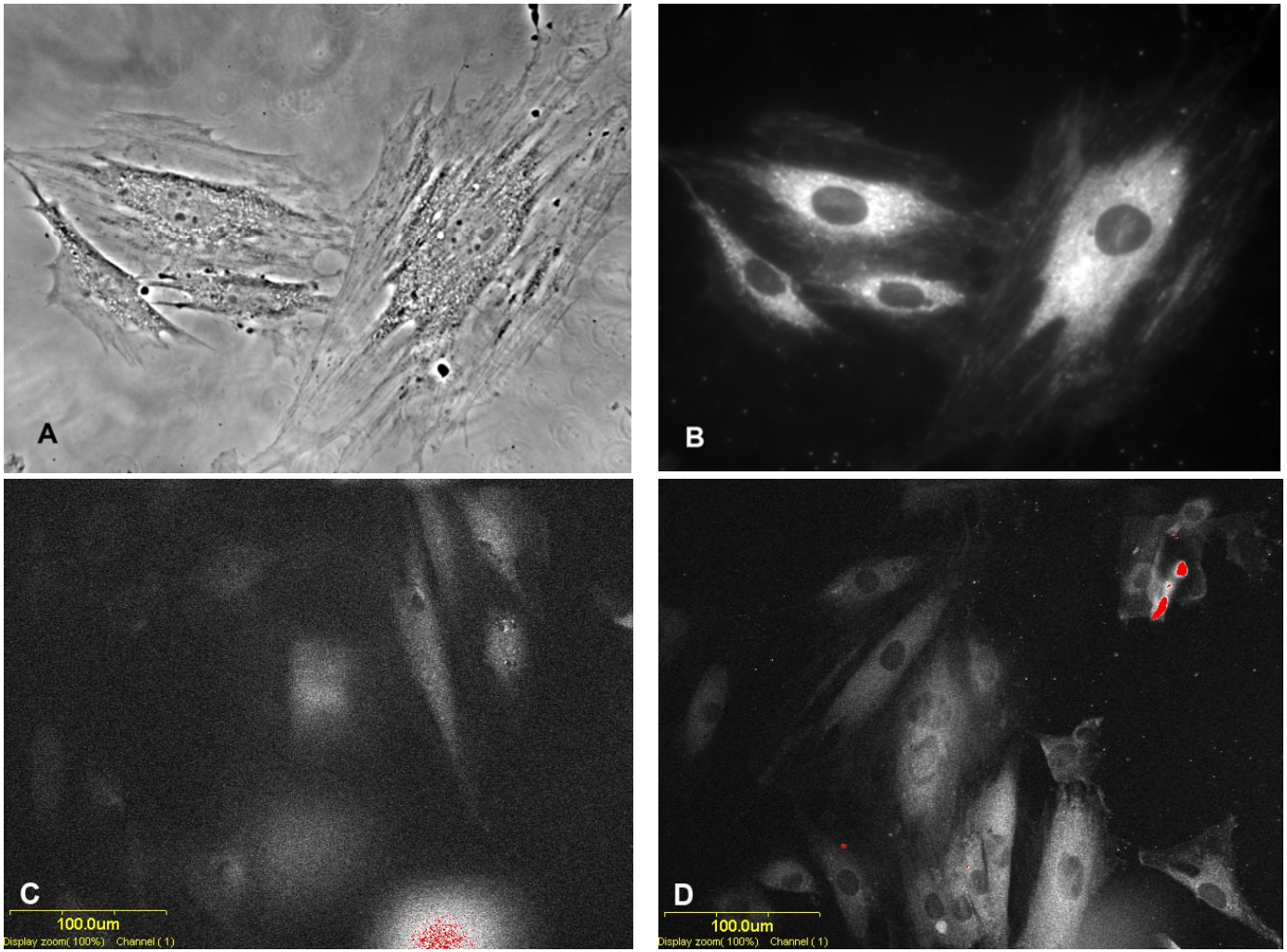

Figure 18.13 (a) Bright field transmission and (b) epi-fluorescent microscopy images (40x) of H9c2 cells stained with a two-photon absorbing probe **15**. Two-photon induced fluorescence microscope images (40×) of (c) control containing no fluorophore and exhibiting some autofluorescence and (d) cells stained with fluorene **15** upon 800 nm fs excitation. Red spots demark signal saturation.

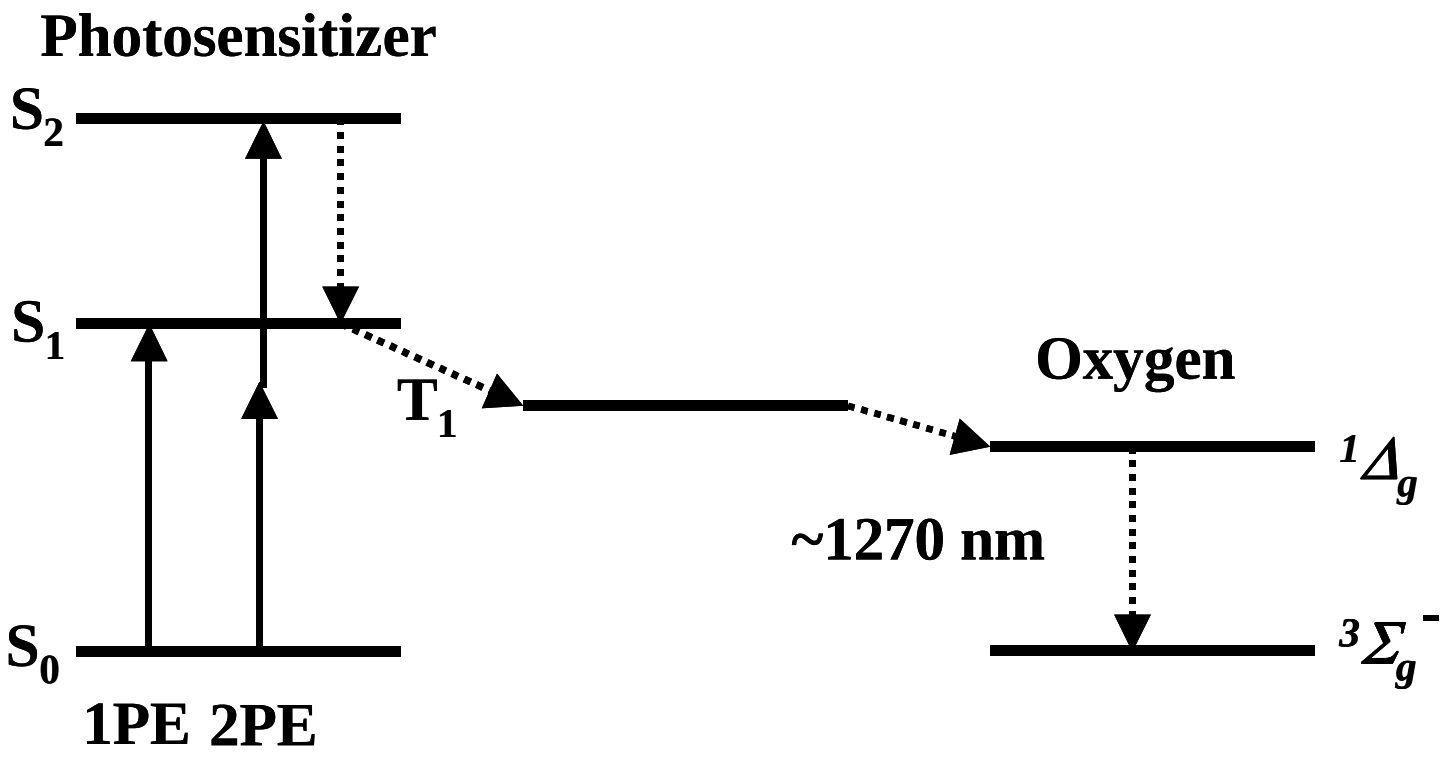

Figure 18.14 Singlet oxygen generation via one-photon excitatio (1PE) or two-photon excitation (2PE).

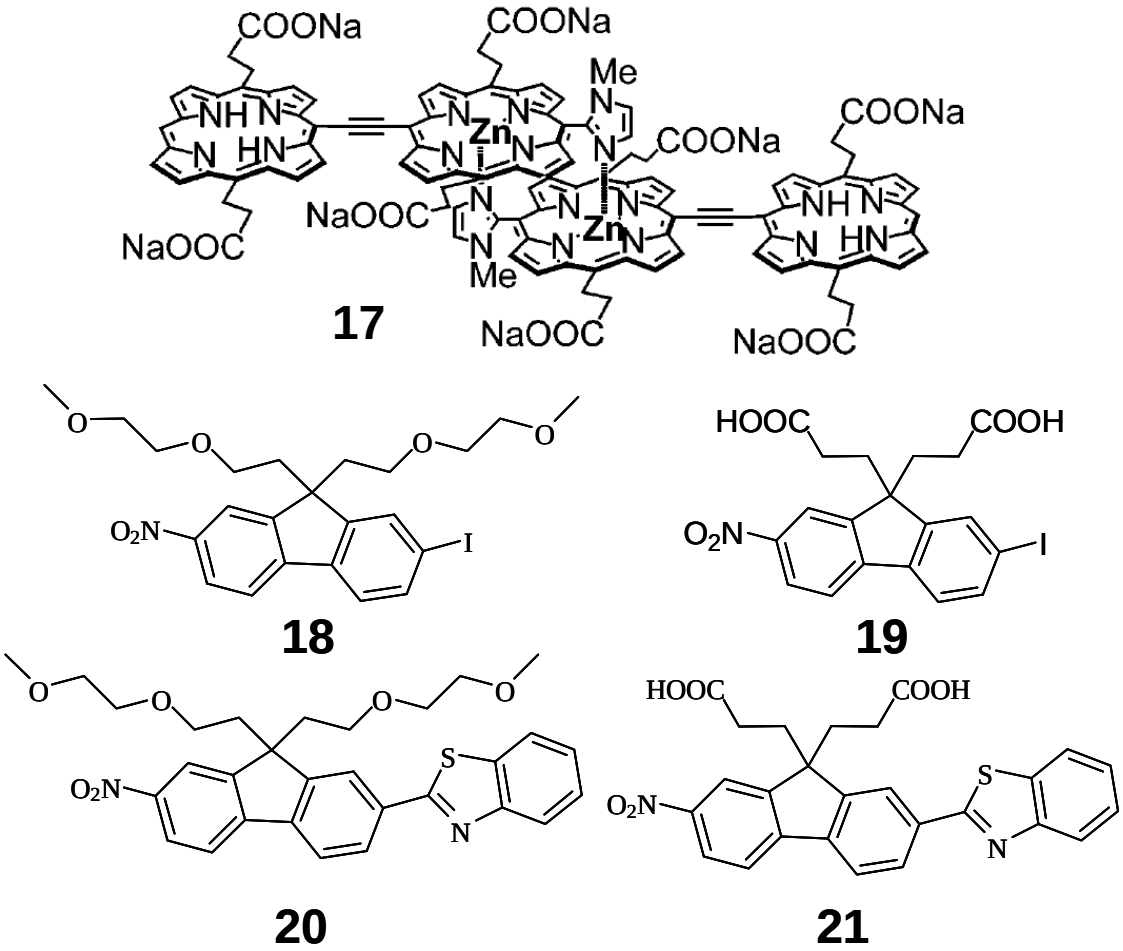

Figure 18.15 Structure of novel two-photon absorption (2PA) photodynamic therapy (PDT) photosensitizers.

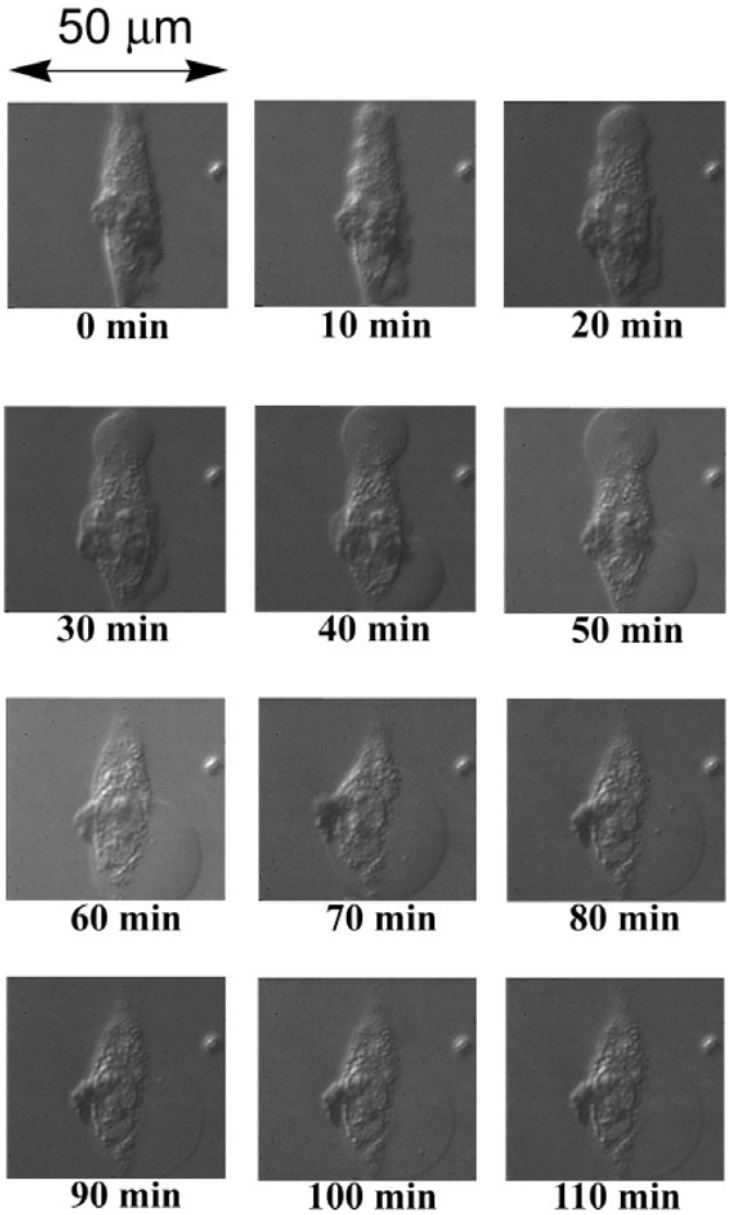

Figure 18.16 Time course of cell death for HeLa cell upon photoirradiation with **17**.

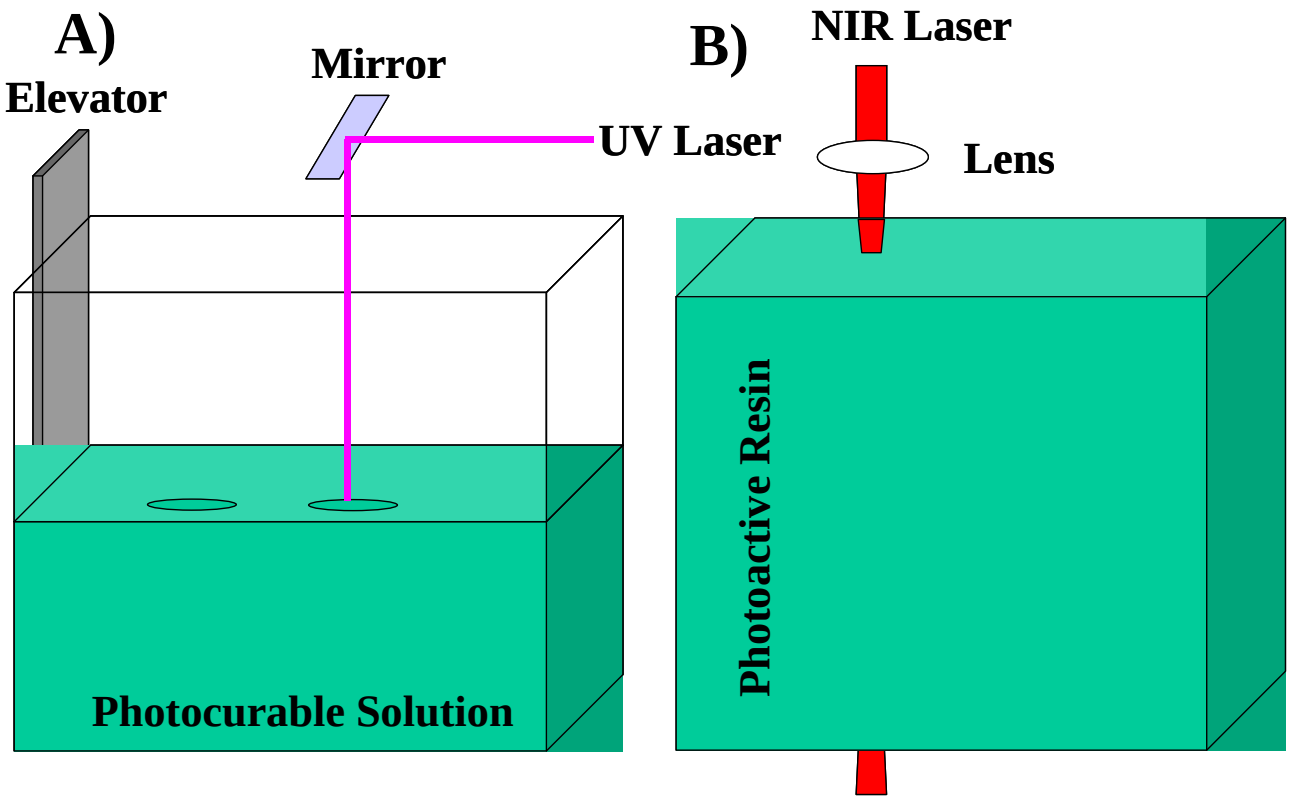

Figure 18.17 (a) Single photon layer-by-layer photostereolithography *vs.* (b) two-photon 3D microfabrication.

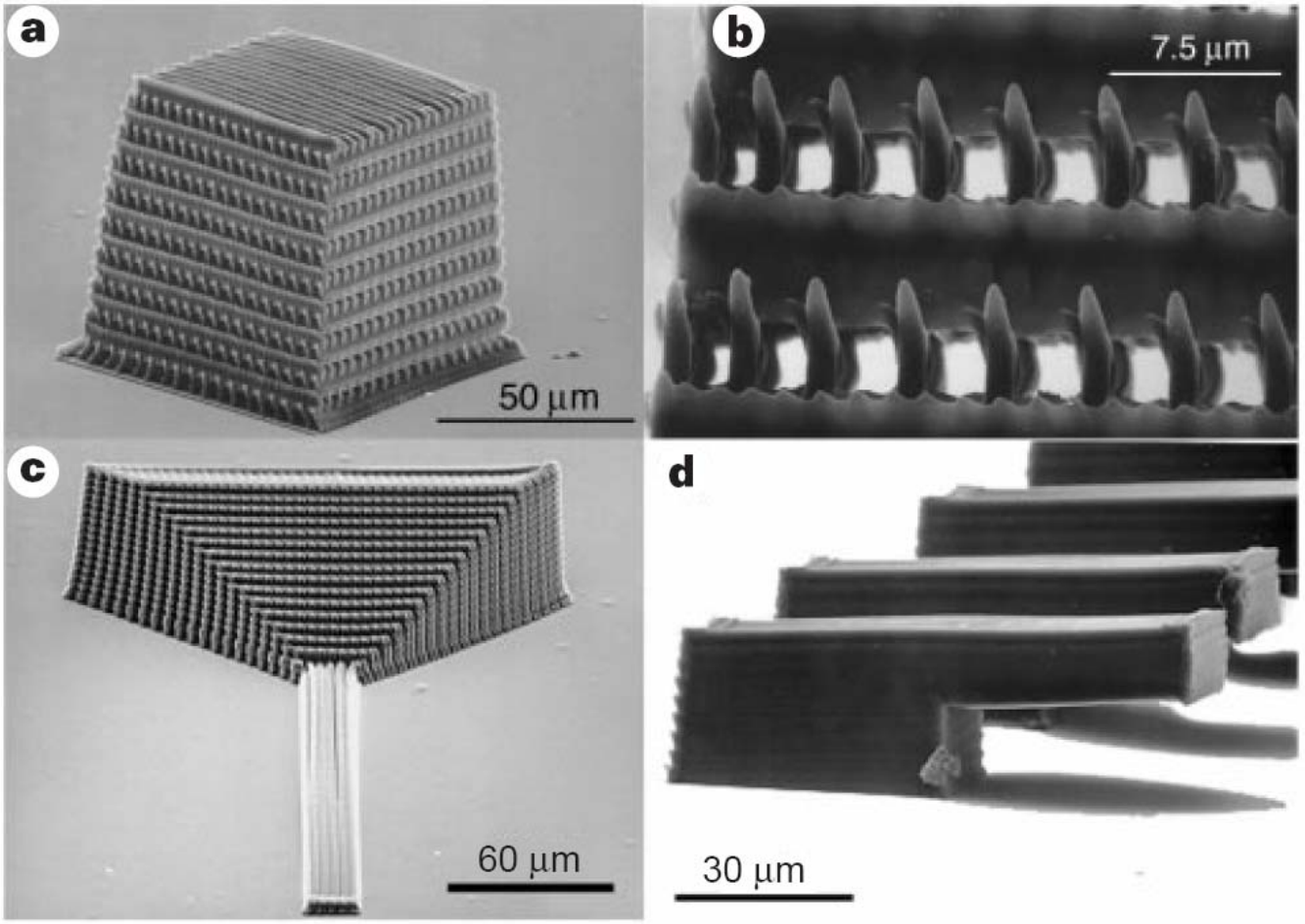

Figure 18.18 Three-dimensional (3D) microstructures produced by two-photon initiated polymerization. (a) Photonic bandgap (PBG) structure. (b) Magnified top-view of structure (c) tapered waveguide structure and (d) array of cantilevers.

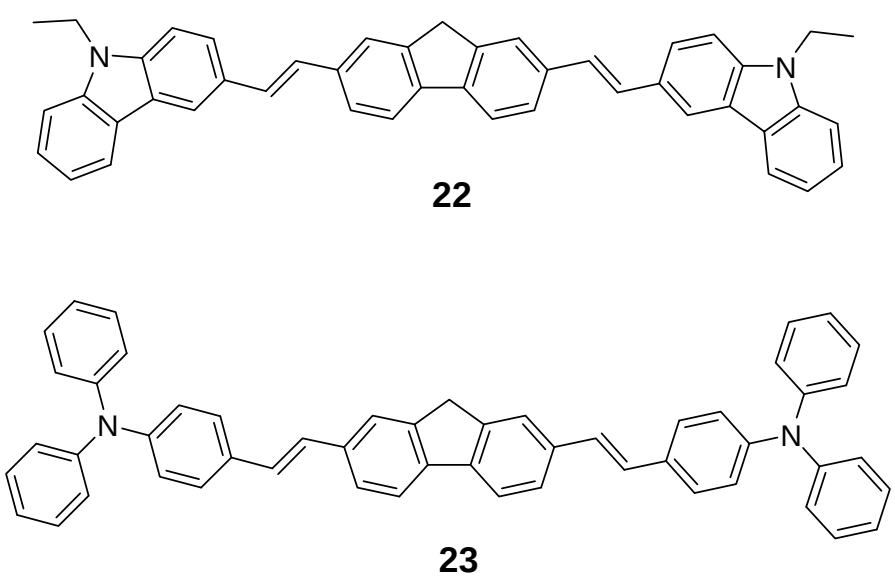

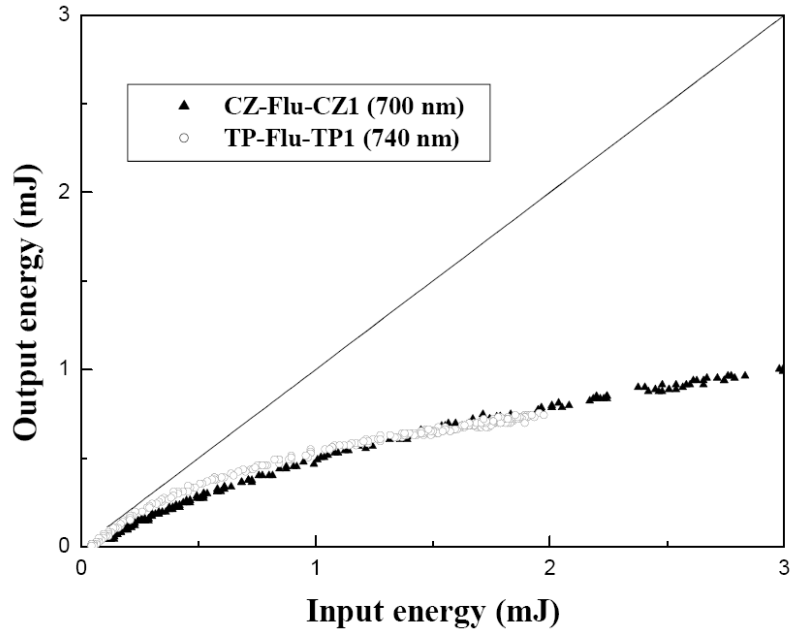

Figure 18.19 Structures of fluorene-based two-photon absorption (2PA) chromophores **22** and **23**, and their optical power limiting properties in THF at 0.005 mol/L.